Protein Science (1998), 7:906–914. Cambridge University Press. Printed in the USA.

The BPI/LBP family of proteins: A structural analysis of conserved regions

LESA J. BEAMER,[1] STEPHEN F. CARROLL,[2] AND DAVID EISENBERG[3]

[1]Biochemistry Department, University of Missouri–Columbia, Columbia, Missouri 65211
[2]XOMA Corporation, 2910 Seventh Street, Berkeley, California 94710
[3]UCLA/DOE Laboratory of Structural Biology, Molecular Biology Institute, UCLA, P.O. Box 951570, Los Angeles, California 90095-1570

(RECEIVED November 3, 1997; ACCEPTED January 13, 1998)

Abstract

Two related mammalian proteins, bactericidal/permeability-increasing protein (BPI) and lipopolysaccharide-binding protein (LBP), share high-affinity binding to lipopolysaccharide (LPS), a glycolipid found in the outer membrane of Gram-negative bacteria. The recently determined crystal structure of human BPI permits a structure/function analysis, presented here, of the conserved regions of these two proteins sequences. In the seven known sequences of BPI and LBP, 102 residues are completely conserved and may be classified in terms of location, side-chain chemistry, and interactions with other residues. We find that the most highly conserved regions lie at the interfaces between the tertiary structural elements that help create two apolar lipid-binding pockets. Most of the conserved polar and charged residues appear to be involved in inter-residue interactions such as H-bonding. However, in both BPI and LBP a subset of conserved residues with positive charge (lysines 42, 48, 92, 95, and 99 of BPI) have no apparent structural role. These residues cluster at the tip of the NH_2-terminal domain, and several coincide with residues known to affect LPS binding; thus, it seems likely that these residues make electrostatic interactions with negatively charged groups of LPS. Overall differences in charge and electrostatic potential between BPI and LBP suggest that BPI's bactericidal activity is related to the high positive charge of its NH_2-terminal domain. A model of human LBP derived from the BPI structure provides a rational basis for future experiments, such as site-directed mutagenesis and inhibitor design.

Keywords: bactericidal proteins; homology modeling; LPS-binding; X-ray crystallography

The related mammalian proteins BPI and LBP function in the host response to Gram-negative bacterial infections. These two 456-residue proteins effect the inflammatory response to a highly toxic bacterial product, lipopolysaccharide (LPS), also known as endotoxin. LPS is a phosphorylated glycolipid uniquely produced by Gram-negative bacteria where it is a critical component of their outer membrane (Raetz, 1996). When present in the bloodstream of mammals, bacteria and their LPS trigger a general inflammatory response. This response is usually protective; however, under certain conditions it can overwhelm the host, leading to septic shock and death (Camussi et al., 1995).

LBP is a serum protein produced constitutively by hepatocytes, and at higher levels during the acute phase response. LBP binds to LPS and transports it to CD14, a membrane-linked receptor on the surface of macrophages and other cells of the immune system (Wright et al., 1990). Binding of the LBP/LPS complex to CD14 increases the host's sensitivity to LPS by two orders of magnitude. LBP has also been shown to transfer LPS to a soluble form of CD14 (sCD14) (Pugin et al., 1993) and to HDL (Wurfel et al., 1994) and phospholipid vesicles (Schromm et al., 1996), which may contribute to its removal from sera.

LBP is related in both sequence (45% amino acid identity) and function to bactericidal/permeability-increasing protein (BPI). Both LBP and BPI bind to LPS (Tobias et al., 1988; Gazzano-Santoro et al., 1992) and are part of the innate immune response. However, unlike LBP, BPI is an intracellular protein found in cytoplasmic granules of polymorphonuclear neutrophils (Weiss & Olson, 1987). BPI is potently bactericidal, targeting Gram-negative bacteria that have been endocytosed by the neutrophil. When added to the bloodstream, BPI and bioactive NH_2-terminal BPI proteins are bactericidal, and can bind to, clear, and neutralize LPS (Elsbach & Weiss, 1995), preventing the inflammatory response triggered by bacteria and their endotoxin. Thus, these two related proteins have opposing effects; when LBP binds to LPS in vivo, it upregulates the immune response, whereas BPI diminishes it.

The three-dimensional structure of BPI was recently determined in our laboratory at 2.4 Å (Beamer et al., 1997), and revealed that the protein had an unusual "boomerang" shape formed by two similar domains with a novel protein fold. In the crystal structure,

Reprint requests to: David Eisenberg, UCLA/DOE Laboratory of Structural Biology, Molecular Biology Institute, UCLA, P.O. Box 951570, Los Angeles, California 90095-1570; e-mail: david@mbi.ucla.edu.

two apolar binding pockets were discovered, each holding a molecule of phosphatidylcholine, a zwitterionic phospholipid. BPI interacts primarily with the acyl carbons chains of the phospholipid, and, because both phosphatidylcholine and LPS have acyl carbon chains, we proposed that LPS (or some portion of it) might also bind in these apolar pockets.

The BPI structure provides a framework to better understand the functional similarities and differences between BPI and LBP. Using this structure, we analyzed the location and potential structural roles of highly conserved residues in these two proteins. We have also constructed a homology model of LBP to examine the distribution of charged residues on the protein surface and to compare regions of potential functional significance in the two proteins.

Results and discussion

The conserved residues of the BPI/LBP family have been analyzed in terms of their location in the molecule, side-chain chemistry (polar, apolar, charged) and solvent accessibility, and possible structural roles. In the following sections, we make two standard assumptions: (1) residues and/or properties that have been conserved evolutionarily are likely to be important for conserved functions, such as LPS binding or structural integrity; and (2) residues/properties that are not conserved between BPI and LBP may correlate with functional differences. A brief description of the BPI structure is included in the legend of Figure 1A. In the following discussion, residue numbers refer to the human BPI sequence.

A

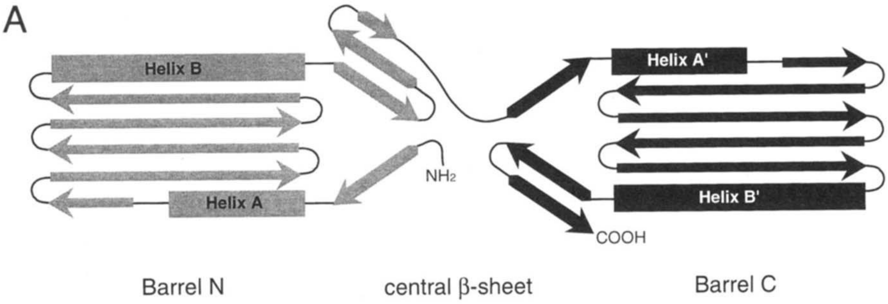

B

```
            1                                                      51                                                    100
BPI human   VNPGVVVRIS QKGLDYASQQ GTAALQKELK RIKIPDYSDS FKIKHLGKGH YSFYSMDIRE FQLPSSQISM VPNVGLKFSI SNANIKISGK WKAQKRFLKM
BPI rabbit  TNPGFTTRIS QKGLDYACQQ GVAVLQKELE KIRIPDVSGK FKLRPFGKGH YNFHSLVVRS FQLPNPQIRL QPNVGLRVSI SNANVRIGGR WKARKGFIKV
BPI bovine  TNPGIVARIT QKGLDYACQQ GVLTLQKELE KITIPNFSGN FKIKYLGKGQ YSFFSMVIQG FNLPNSQIRP LPDKGLDLSI RDASIKIRGK WKARKNFIKL
LBP human   ANPGLVARIT DKGLQYAAQE GLLALQSELL RITLPDFTGD LRIPHVGRGR YEFHSLNIHS CELLHSALRP VPGQGLSLSI SDSSIRVQGR WKVRKSFFKL
LBP rat     VNPAMVVRIT DKGLEYAAKE GLLSLQRELY KITLPDFSGD FKIKAVGRGQ YEFHSLEIQS CQLRGSSLKP LPGRGLSLSI SDSSISVRGK WKVRRSFVKL
LBP mouse   VNPGVVARIT DKGLAYAAKE GLVALQRELY KITLPDFSGD FKIKAVGRGQ YEFHSLEIQN CELRGSSLKL LPGQGLRLAI SDSSIGVRGK WKVRKSFLKL
LBP rabbit  TNPGLITRIT DKGLEYAARE GLLALQRKLL EVTLPDSDGD FRIKHFGRAQ YKFYSLKIPR FELLRGTLRP LPGQGLSLDI SDAYIHVRGS WKVRKAFLRL

            101                                                    151                                                   200
BPI human   SGNFDLSIEG MSISADLKLG SNPTSGKPTI TCSSCSSHIN SVHVHISKSK VGWLIQLFHK KIESALRNKM NSQVCEKVTN SVSSELQPYF QTLPVMTKID
BPI rabbit  RGKFDLSVEG VSISADLKLG SVPASGRATV TCSSCSSNIN RARLRSQASW GGWLEKLFHK RIESSLRNTM NSKICQVLTS SVSSKLQPYV ETLPLKERLD
BPI bovine  GGNFDLSVEG ISILAGLNLG YDPASGHSTV TCSSCSSGIN TVRIHISGSS LGWLIQLFRK RIESLLQKSM TRKICEVVTS TVSSKLQPYF QTLPVTTKLD
LBP human   QGSFDVSVKG ISISVNLLLG SES-SGRPTV TASSCSSDIA DVEVDMSGD- LGWLLNLFHN QIESKFQKVL ESRICEMIQK SVSSDLQPYL QTLPVTTEID
LBP rat     HGSFDLDVKS VTISVDLLLG VDP-SERPTV TASGCSNRIR DLELHVSGN- VGWLLNLFHN QIESKLQKVL ESKICEMIQK SVTSDLQPYL QTLPVTADID
LBP mouse   HGSFDLDVKG VTISVDLLLG MDP-SGRPTV SASGCSSRIC DLDVHISGN- VGWLLNLFHN QIESKLQKVL ENKVCEMIQK SVTSDLQPYL QTLPVTAEID
LBP rabbit  KNSFDLYVKG LTISVHLVLG SES-SGRPTV TTSSCSSDIQ NVELDIEGD- LEELLNLLQS QIDARLREVL ESKICRQIEE AVTAHLQPYL QTLPVTTQID

            201                                                    251                                                   300
BPI human   SVAGINYGLV APPATTAETL DVQMKGEFYS ENHHNPPPFA PPVMEFPAAH DRMVYLGLSD YFFNTAGLVY QEAGVLKMTL RDDMIPKESK FRLTTKFFGT
BPI rabbit  SVAGIDYSLV APPRATADSL DMQLKGEFYN VARPSPPPFM PPPMAIPSLH DRMIYLAISD YLFNTAALVY QQAGAFGLTL RDDMIPKESK SRLTTKFLGK
BPI bovine  KVAGVDYSLV APPRATANNL DWLLKGEFFS LAHRSPPPFA PPALAFPSDH DRMVYLGISE YFFNTAGFVY QKAGALNLTL RDDMIPKESK FRLTTKFFGI
LBP human   SFADIDYSLV EAPRATAQML EVMFKGEIFH RNHRSPVTLL AAVMSLPEEH NKMVYFAISD YVFNTASLVY HEEGYLNFSI TDDMIPPDSN IRLTTKSFRP
LBP rat     TILGIDYSLV AAPQAKAQTL DVMFKGEIFN RNHRSPVTTP TPTMSLPEDS KQMVYFAISD QAFNIATRVY HQAGYLNFTI TDDMLPPDSN IRLNTKAFRP
LBP mouse   NVLGIDYSLV AAPQAKAQVL DVMFKGEIFN RNHRSPVATP TPTMSLPEDS KQMVYFAISD HAFNIASRVY HQAGYLNFSI TDDMLPHDSG IRLNTKAFRP
LBP rabbit  SFAGIDYSLM EAPRATAGML DVMFKGEIFP LDHRSPVDFL APAMNLPEAH SRMVYFSISD YVFNTASLAY HKSGYWNFSI TDAMVPADLN IRRTTKSFRP

            301                                                    351                                                   400
BPI human   FLPEVAKKFP NMKIQIHVSA STPPHLSVQP TGLTFYPAVD VQAFAVLPNS SLASLFLIGM HTTGSMEVSA ESNRLVGELK LDRLLLELKH SNIGPFPVEL
BPI rabbit  ALPQVAKMFP NMNVQLTLSV SSPPHLTTRP TGIALTAAVD LQAFAILPNS SLASLFLLGL KLNTSAKIGT KADKLVGELT LGRLILELKH SNIGSFPVQL
BPI bovine  LIPQVAKMFP DMQMQLFIWA SLPPKLTMKP SSLDLIFVLD TQAFAILPNS SLDPLFLLEM NLNLSVVVGA KSDRLIGELR LDKLLLELKH SDIGPFSVES
LBP human   FVPRLARLYP NMNLELQGSV PSAPLLNFSP GNLSVDPYME IDAFVLLPSS SKEPVFRLSV ATNVSATLTF NTSKITGFLK PGKVKVELKE SKVGLFNAEL
LBP rat     FTPLITRKYP DMNLELLGTV VSAPLLNVSP GNLSLAPQME IEGFVILPSS ARESVFRLGV VTNVFVSLTF DNSKVTGMLH PEKAQVRLIE SKVGMFNVNL
LBP mouse   FTPQIYKKYP DMKLELLGTV VSAPILNVSP GNLSLAPQME IEGFVILPTS AREPVFRLGV VTNVFASLTF NNSKVTGMLH PDKAQVRLIE SKVGMFNVNL
LBP rabbit  FVPLLANLYP NMNLELQGTV NSEQLVNLST ENLLEEPEMD IEALVVLPSS AREPVFRLGV ATNVSATLTL NTRKITGFLK PGRLQVELKE SKVGGFNVEL

            401                                                    451
BPI human   LQDIMNYIVP ILVLPRVNEK LQKGFPLPTP ARVQLYNVVL QPHQNFLLFG ADVVYK
BPI rabbit  LQALMDYVLS AVVLPKVNEK LQRGLPLPMP RKVQLYDLVL QPHQDFLLLG ANVQHG
BPI bovine  LQSVINYVMP TIVLPVINKK LQKGFPLPLP AYIELFNLTL QPYQDFLLFG ADVQYS
LBP human   LEALLNYYIL NTFYPKFNDK LAEGFPLPLL KRVQLYDLGL QIHKDFLFLG ANVQYMRV
LBP rat     FQAFLNYYLL NSLYPDVNDE LAKGFPLPLP RRIKLHDLDF QIHKNFLYLG ANVQYMRV
LBP mouse   FQAFLNYYLL NSLYPDVNAE LAQGFPLPLP RHIQLHDLDF QIRKDFLYLG ANVQYMRV
LBP rabbit  LEALLNYYIL NNLYPKVNEK LAHRFPLPLL RHIQLYDLLL QTHENFLLVG ANIQYRRV
```

Fig. 1. A: Schematic diagram of BPI showing the elongated shape and emphasizing its pseudosymmetry. Elements of the NH_2-terminal domain (residues 1–229) are shown in gray, and the COOH-terminal domain (residues 251–456) in black. Strands are indicated by arrows and helices are shown as rectangles. The two domains form three structural elements—the NH_2-terminal barrel (barrel N), a central β-sheet, and the COOH-terminal barrel (barrel C). Each barrel is composed of two α-helices (helices A and B in barrel N and A′ and B′ in barrel C) and a twisted β-sheet. Barrel N extends from residues 10–193; barrel C includes residues 260–426. The remaining residues form the central β-sheet, except for residues 230–250, which make up a proline-rich linker between the two domains. The two apolar binding pockets are situated near the interfaces between each barrel and the central sheet. **B:** Sequence alignment of the three known BPI and four known LBP sequences (SWISS-PROT accession numbers: BPI_HUMAN P17213, BPI_BOVIN P17453, BPI_RABIT Q28739, LBP_HUMAN P18428 (Theofan et al., 1994), LBP_RABIT P17454, LBP_MOUSE Q61805, LBP_RAT Q63313). Alignment was performed with CLUSTAL W (Higgins & Sharp, 1989). Identical residues are indicated by *. The two one-residue gaps in LBP are indicated with a dash.

An alignment of the seven known BPI and LBP sequences (Fig. 1B) shows an obvious evolutionary relationship between the proteins. Of the 456 residues, 102 are identical in all seven proteins (22% identity overall) and occur throughout the amino acid sequence. Based on the BPI model, many of these residues fall in structurally important locations in the protein, such as near turns or loops. Residues with unusual backbone flexibility (Gly) or rigidity (Pro) are also highly conserved. All members of the family share the single conserved disulfide bond (Cys132 and Cys175) that anchors helix B to the β-sheet of barrel N. From the three-dimensional model, no other disulfide bonds are expected in the family members with additional cysteines.

Location of conserved residues

Of the 102 strictly conserved residues, 46 are in barrel N, 28 are in barrel C, and 26 are in the central β-sheet (excluding the linker region). This means that barrel N (182 residues) is 25% conserved, barrel C (164 residues) is only 17% conserved, and the central sheet (90 residues excluding the linker) is 31% conserved. Although the conserved residues fall throughout the amino acid sequence, highlighting their location on the BPI structure (Fig. 2A) shows that they tend to fall in the center of the protein, near the interfaces between the two barrels and the central β-sheet. These residues presumably play important roles in maintaining the over-

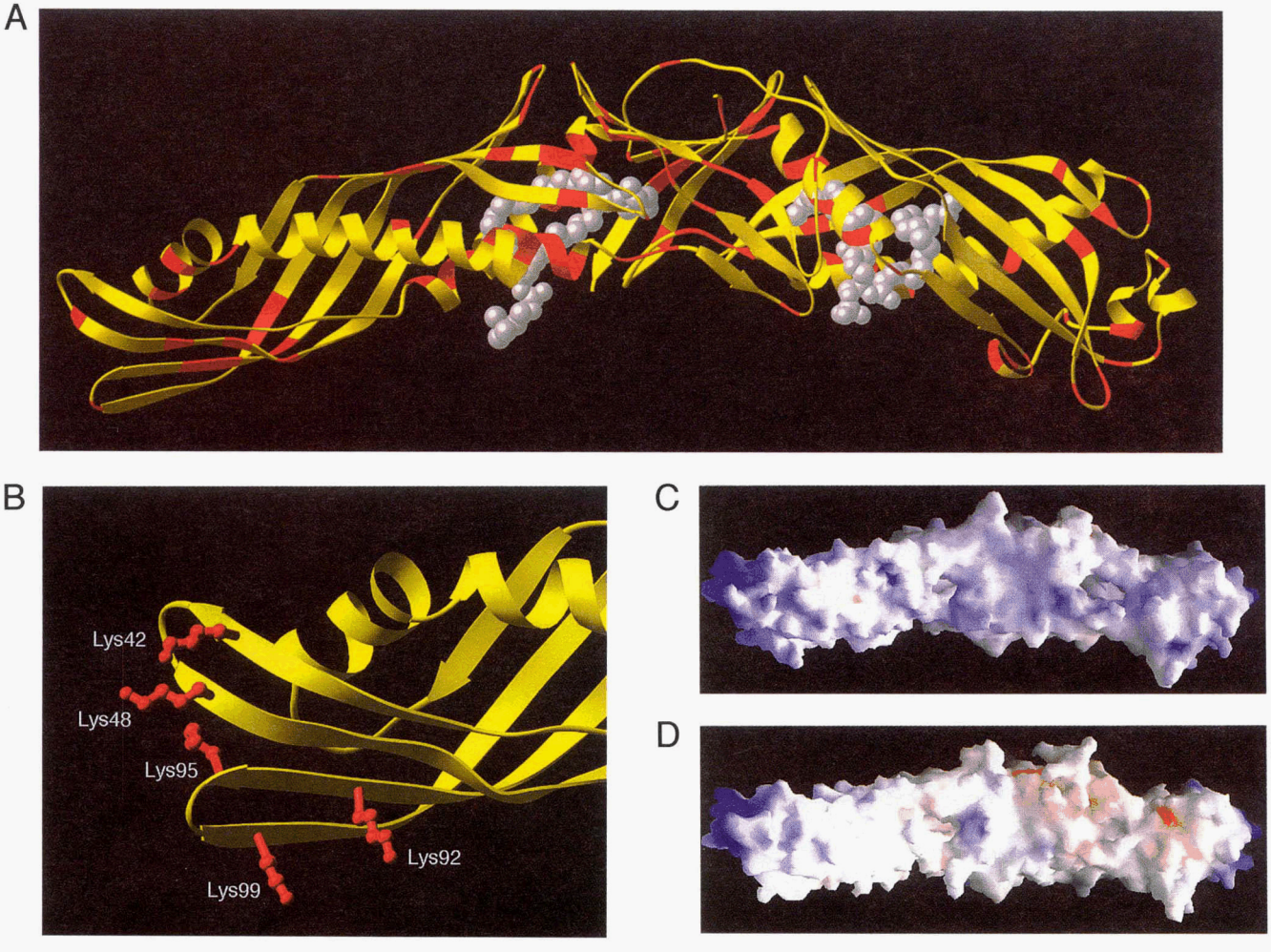

Fig. 2. A: Ribbon diagram (Carson, 1991) of the BPI structure. The NH_2-terminal domain is on the left. Residues that are identical in all BPI and LBP sequences are red; others are yellow. The two bound phosphatidylcholine molecules seen in the BPI crystal structure are shown as space-filling models in silver. Although the red residues fall throughout the protein, many are found in the center of the molecule near the two lipid-binding sites. **B:** Ribbon diagram of BPI's NH_2-terminal domain. Orientation is similar to that in **A**. Side chains for five conserved lysines in the BPI/LBP family (residues 42, 48, 92, 95, and 99) are shown in red. Unlike other charged residues in BPI, these residues do not make inter-residue interactions in the structure and may be involved in electrostatic interactions with negatively charged LPS molecules. Figure prepared by RIBBONS (Carson, 1991). **C:** Electrostatic surfaces of human BPI, and **D:** Human LBP calculated by GRASP (Nicholls et al., 1991). Negative potential is shown in red, positive potential in blue. Orientation is the same for both proteins and the view is into the lipid binding pockets (protein has been rotated approximately 90° about its long axis from view in **A**). The NH_2-terminal domain is on the left; the phospholipid has been excluded from the model. Notice the high concentration of positive charge on BPI, particularly in its NH_2-terminal domain.

all architecture of the protein and the spatial arrangement of the two barrels and central sheet. Because the lipid-binding pockets are found in the same area of the protein, this suggests that much of the structure of the protein is dedicated to preserving these pockets. Nineteen of these completely conserved residues are directly involved in forming the pockets (a side-chain atom lies within 4 Å of a lipid atom or shows a change in solvent accessible surface area when the lipid is removed from the structure). It is noteworthy that these regions are also the most structurally conserved between the NH_2- and COOH-terminal domains of BPI (L.J. Beamer & D. Eisenberg, unpubl.), further suggesting their functional relevance.

Mapping the conserved residues on the three-dimensional structure also highlights the fact that the NH_2-terminal domains of the BPI/LBP family are more conserved than the COOH-terminal domains, consistent with known function. The NH_2-terminal domains of BPI and LBP are similar in function, both showing high affinity binding to LPS. On the other hand, it is believed that the COOH-terminal domain of LBP interacts with the CD14 receptor (Han et al., 1994), while it has been reported that the COOH-terminal domain of BPI promotes bacterial phagocytosis by neutrophils (Iovine et al., 1997) and has some endotoxin-neutralizing activity (Ooi et al., 1991; Abrahamson et al., 1997). One stretch of residues (315–375) in the COOH-terminal domain is rather divergent in sequence. This corresponds to several strands of barrel C, an area generally on the opposite side of the protein as the lipid-binding pockets. It is possible that residues in this area of LBP interact with CD14, a hypothesis that could be tested by site-directed mutagenesis.

Side-chain chemistry

Most of the strictly conserved residues in the BPI/LBP family are apolar (Table 1): 68 of the 102 conserved residues fall in this

Table 1. *Strictly conserved apolar residues in the BPI/LBP family*[a]

Residue				Solvent		Residue				Solvent	
BPI[b]	LBP[c]	Location		accessible?[d]	Pocket?	BPI[b]	LBP[c]	Location		accessible?[d]	Pocket?
Pro3	—	Central sheet	Turn before strand	Y		Leu209	207	Central sheet	Strand	N	
Ile9	—	Barrel N	Strand	N	Y	Pro213	211	Central sheet	Strand at bulge	N	
Gly13	—	Barrel N	Helix A	N	Y	Ala217	215	Central sheet	Turn	Y	
Leu14	—	Barrel N	Helix A	N	Y	Leu220	218	Central sheet	Strand	N	Y
Ala17	—	Barrel N	Helix A	N	Y	Gly226	224	Central sheet	Strand at bulge	N	
Gly21	—	Barrel N	Helix A	N	Y	Pro236	234	Linker		Y	
Leu25	—	Barrel N	Helix A	N	Y	Pro247	245	Linker		Y	
Leu29	—	Barrel N	Helix A	N		Met253	251	Central sheet	Strand	Y	
Pro35	—	Barrel N	Coil	Y		Phe263	261	Barrel C	Helix A′	N	Y
Gly47	—	Barrel N	Strand after turn	Y		Ala266	265	Barrel C	Helix A′	N	
Phe53	—	Barrel N	Strand before bulge	N		Gly274	272	Barrel C	Coil	Y	
Leu63	—	Barrel N	Strand before bulge	N		Met284	282	Barrel C	Loop	Y	
Pro72	—	Barrel N	Turn	Y		Pro286	284	Barrel C	Loop	Y	
Gly75	—	Barrel N	Strand	N		Pro303	301	Barrel C	Loop	Y	
Leu76	—	Barrel N	Strand	N	Y	Pro310	308	Barrel C	Loop	Y	
Ile80	—	Barrel N	Strand	N		Met312	310	Barrel C	Loop	Y	
Gly89	—	Barrel N	Strand at bulge	N		Leu347	345	Barrel C	Turn	Y	
Phe97	—	Barrel N	Turn	Y		Pro348	346	Barrel C	Turn	Y	
Phe104	—	Barrel N	Strand	N		Phe356	354	Barrel C	Strand at bulge	N	
Ile113	—	Barrel N	Strand	N		Gly377	375	Barrel C	Strand	N	Y
Leu117	—	Barrel N	Strand	N	Y	Leu379	377	Barrel C	Strand	N	Y
Leu119	—	Barrel N	Strand	N	Y	Leu388	387	Barrel C	Strand	Y	
Gly120	—	Barrel N	Strand before turn	Y		Gly394	392	Barrel C	Loop before helix B′	Y	
Cys135	134	Barrel N	Strand, disulfide	Y		Phe396	394	Barrel C	Loop before helix B′	Y	
Ile139	138	Barrel N	Strand	N		Pro415	413	Barrel C	Helix B′	Y	
Leu154	152	Barrel N	Helix B	N		Leu421	419	Barrel C	Helix B′	N	Y
Leu157	155	Barrel N	Helix B	Y		Pro426	424	Barrel C	Coil	Y	
Ile162	160	Barrel N	Helix B	N		Leu427	425	Central sheet	Coil	Y	
Cys175	173	Barrel N	Helix B, disulfide	Y		Pro428	426	Central sheet	Coil	N	
Val182	180	Barrel N	Helix B	N	Y	Leu435	433	Central sheet	Strand	N	Y
Leu186	184	Barrel N	Helix B	N	Y	Phe446	444	Central sheet	Strand	Y	
Pro188	186	Barrel N	Helix B	Y		Leu447	445	Central sheet	Strand	N	
Leu193	191	Barrel N	Coil	N		Gly450	448	Central sheet	Strand	N	
Pro194	192	Barrel N	Coil	Y		Ala451	449	Central sheet	Strand	N	

[a]Most of these residues are solvent inaccessible, and they tend to cluster near the lipid binding pockets.
[b]Residues of the human BPI sequence.
[c]Residue numbers for human LBP when different from BPI.
[d]Solvent accessibility was calculated with X-PLOR (Brunger, 1990). Residues with less than 5 $Å^2$ of exposed surface area were classified as buried.

category, and include the 19 residues mentioned above that participate in forming the apolar lipid binding pockets. Except for glycines and prolines, most of these residues are solvent inaccessible and are buried in the hydrophobic core of the protein. Despite the pockets, each barrel has a substantial hydrophobic core, formed by packing of the two helices against the twisted sheet. Apolar residues that are not buried include several phenylalanines (97, 396, 446), leucines (427, 388, 347, 157), methionines 284 and 312, and Ala217. Most of these residues are in the relatively hydrophobic COOH-terminal domain, and are found in loops or turns, increasing their solvent accessibility.

Conserved charged and polar residues in the BPI family are involved in multiple inter-residue interactions. Twenty-three polar residues and 10 charged residues are strictly conserved (Tables 2 and 3). Most of these residues appear to make interactions with other residues of the protein, including salt bridges and side chain–side chain or side chain–backbone H-bonds. However, given the medium (2.4 Å) resolution of the BPI structure, it cannot be stated with certainty that a particular residue interacts with another. Therefore, the described interactions are based solely on reasonable interaction distances between the residue pairs. Potential interactions with solvent molecules were not considered as part of this analysis.

Table 2 details the conserved polar residues found in the BPI/LBP family. The vast majority of the side chains of these residues make H-bonds with backbone atoms in the protein. This type of side chain–backbone interaction, where one partner is basically immobile, has fewer degrees of freedom than side chain–side chain interactions where both are free to move. Therefore, these residues may play critical roles in maintaining the tertiary structure of the protein by, for example, linking secondary structural elements together. A number of instances of this are seen in Table 2, including interactions between β-strands, between a helix and a strand, and between the barrels and central sheet. Two interesting cases are found in barrel C where an asparagine from each helix makes a bidentate interaction with the backbone atoms of an adjacent barrel strand. One of these residues, Asn264 from helix A′, forms a H-bond to the backbone amide and carbonyl of Leu 326 on the second strand of the barrel. On helix B′, Asn418 forms a bidentate H-bond with the backbone atoms of Leu379 from the final strand of barrel C. These bidentate interactions require that the side chain is both a H-bond donor and acceptor, explaining why it is highly conserved.

Only two of the strictly conserved polar/charged residues fall near the entrance of a lipid-binding pocket, Asp200 and Tyr270. However, neither of these two residues seems to be directly involved in lipid binding; rather they interact with each other. Tyr270 is found on helix A′ of barrel C, and Asp200 is found in a turn of the central β-sheet which approaches the COOH-terminal lipid binding pocket. Asp200 stabilizes this turn by making two H-bonds with backbone atom of residues 202 and 203. It also interacts with Tyr270 at end of helix A′, linking barrel C to the central β-sheet. These two residues appear to be conserved for structural reasons, rather than direct protein–lipid interactions. Overall, it seems that the residues at the entrances of the pockets are more variable than

Table 2. *Strictly conserved polar residues in the BPI/LBP family*[a]

Residue				
BPI[b]	LBP[c]	Location		Interactions[d]
Asn2	—	Central sheet	Coil	bb H-bond to Pro241, connects N-terminus to linker
Tyr16	—	Barrel N	Helix A	bb H-bond to Tyr455, links helix A to central sheet
Gln26	—	Barrel N	Helix A	—
Tyr51	—	Barrel N	Strand	—
Ser55	—	Barrel N	Strand	—
Trp91	—	Barrel N	Strand	bb H-bond to Gly102 and Asn103, links neighboring strands
Ser125	124	Barrel N	Loop	sc H-bond to Asn122
Thr129	128	Barrel N	Strand	bb H-bond to Gly120; helps hold two strands together
Ser133	132	Barrel N	Strand at bulge	—
Ser136	135	Barrel N	Strand	—
Gln187	185	Barrel N	Helix B	bb H-bond to Ile130; connects helix B to sheet
Tyr189	187	Barrel N	Helix B	bb H-bond to Ala431; connects helix B to central sheet
Thr192	190	Barrel N	Coil	bb H-bond to Tyr189, Ala431; connects helix B to central sheet and helps terminate helix
Tyr207	205	Central sheet	Strand	bb H-bond to Pro426, holds together N- and C-terminal domains
Tyr255	253	Central sheet	Strand	—
Ser259	257	Central sheet	Strand	bb H-bond to Gly4, stabilizes central sheet
Asn264	262	Barrel C	Helix A′	bb H-bond to Leu326, Asp260; bidentate interaction from helix A′ to sheet
Tyr270	268	Barrel C	Helix A′	H-bond to sc of Asp200; near C-pocket entry
Ser350	348	Barrel C	Loop	Mutated to Ala
Ser391	389	Barrel C	Loop	bb H-bond to Gly394
Tyr407	405	Barrel C	Helix B′	—
Asn418	416	Barrel C	Helix B′	bb H-bond to Leu379; bidentate interaction from helix B′ to sheet
Gln441	439	Central sheet	Strand	—

[a]Most of the conserved polar residues are involved in inter-residue interactions such as H-bonding.
[b]Residues of the human BPI sequence
[c]Residue numbers for human LBP when different from BPI.
[d]Table includes all side chains with at least one atom that can form an H-bond and does not include charged residues (see Table 3). bb stands for backbone, sc for side chain. Distance cutoff for proposed interactions is 3.2 Å.

Table 3. *Conserved charged residues in the BPI/LBP family*[a]

Residue				
BPI[b]	LBP[c]	Location		Interactions[d]
Arg8	—	Central sheet	Strand	Salt bridge with **Asp221**, sc H-bond to Thr219, bb H-bond to Phe246 holds together beginning and end of N-terminal domain, stabilizes central β-sheet
Lys12	—	Barrel N	Helix A	Salt bridge with Asp451, links C-terminal to N-terminal domain
Lys42[e]	—	Barrel N	Strand	—
Lys48[e]	—	Barrel N	Strand	—
Lys92	—	Barrel N	Strand	—
Lys95[e]	—	Barrel N	Strand	—
Lys99[e]	—	Barrel N	Strand	—
Asp105	—	Barrel N	Strand	sc H-bond to Ser88
Glu163[e]	161	Barrel N	Helix B	sc H-bond to Arg167 and His159; may help stabilize bend in helix
Asp200	198	Central sheet	Turn	sc H-bond to **Tyr270**, bb H-bond to 202, 203; at pocket entry
Asp221[e]	Glu219	Central sheet	Strand	Salt bridge to **Arg8**; sc H-bond with Thr219
Lys225	223	Central sheet	Strand	Salt bridge to **Glu227**
Glu227	225	Central sheet	Strand	Salt bridge to **Lys225**; sc H-bond to Tyr261 at start of barrel C
Asp260[e]	258	Barrel C	Helix A′	bb H-bond to Tyr261
Asp282	280	Barrel C	Loop	Salt bridge to **Arg292**; bb H-bond to Leu293
Arg292	290	Barrel C	Loop	Salt bridge to **Asp282**; bb H-bond to **Asp282**, **Pro286**
Lys296	294	Barrel C	Loop	Not well defined in structure
Asp340[d]	Glu338	Barrel C	Strand	Salt bridge with Lys389 on back of barrel C

[a]Most of these residues make inter-residue contacts, except for a subset in the NH_2-terminal domain, which may be involved in LPS binding.
[b]Residues of the human BPI sequence.
[c]Residue names and numbers for human LBP when different from BPI.
[d]Residues indicated in bold font under Interactions are strictly conserved.
[e]Indicates that charge is strictly conserved, but not side chain identity.

those that make up their interiors. Because the apolar interiors of the pockets presumably confer little specificity to binding, these pockets may accommodate a variety of apolar ligands.

Because of their potential interactions with the negatively charged LPS molecule, the charged residues of BPI and LBP (particularly the lysines and arginines) are of considerable interest. A closer inspection of the charged residues in the BPI/LBP family reveals 18 that are completely conserved (10 positive and 8 negative), 8 in barrel N, 5 in barrel C, and 5 in the central β-sheet. For this discussion, we consider all residues that have conserved charge rather than only those with identical side chains. An analysis of the roles of the conserved charged residues shows that they fall into two general categories (Table 3). The first group contains residues that are involved in inter-residue interactions and, therefore, appear to have a role in maintaining the structural integrity of the protein. The second category contains residues that have no obvious structural roles and are presumably conserved for functional reasons common to the two proteins, such as LPS binding.

Potential structural roles of the conserved charged residues are detailed in Table 3. One of these, Asp200, is located near the COOH-terminal lipid-binding pocket and was discussed above. Other interactions include three salt bridges where each of the residues involved is strictly conserved. One of these is between Arg8 and Asp221. This interaction appears to hold together the beginning and end of the NH_2-terminal domain, and stabilizes the central β-sheet. The second pair, Glu227 and Lys225, are both in the central β-sheet and this side chain–side chain interaction may serve to keep the intervening residue, a flexible glycine, in the correct conformation. Glu227 also makes a H-bond to Tyr61 at the beginning of helix A′ in barrel C. The third conserved salt bridge is between Asp282 and Arg292, and occurs in a loop in barrel C, one of the areas that differs significantly from its counterpart in barrel N. Another of the charged residues is involved in a potentially important set of interactions in barrel N. It is Glu163 (also Asp), which occurs just after a critical bend in helix B. This bend allows this relatively long helix (40 residues) to pack more tightly against the twisted sheet of barrel N, allowing the formation of a closely packed hydrophobic core. Glu163 makes interactions with the side chains of two relatively conserved residues Arg167 (also Gln) and His159 (also Arg/Gln). This extended network of interactions may help stabilize the bend in helix B, which interrupts the regular helical H-bonding pattern.

The second category of conserved charged residues, those with no apparent structural role, are found exclusively in the NH_2-terminal barrel (Fig. 2B). These five residues (lysines 42, 48, 92, 95, and 99) are solvent exposed and make no apparent interactions with any other residues in the NH_2-terminal domain, which is highly positively charged. None of these residues is near the lipid-binding pockets, a potential site of interaction with LPS. However, previous experiments have indicated a role for several of these residues in LPS binding. For instance, peptides derived from this region of BPI have anti-LPS and antibacterial activity (Little et al., 1994). In addition, site-directed mutagenesis of lysines 95 and 99 of LBP shows a decrease in LPS binding and rate of LPS transfer (Lamping et al., 1996). It, therefore, seems likely that the positively charged residues mentioned above function in LPS recognition or binding, possibly through electrostatic interactions with phosphorylated sugar groups of LPS. Thus, the interaction of BPI

and LBP with LPS appears to be a complex and potentially multistep process, involving several distinct regions of the protein: the patch of positively charged residues described above, the apolar pockets, and perhaps other areas as well. This proposal is consistent with functional evidence for both electrostatic and hydrophobic components of BPI's interaction with the bacterial membrane (Weiss et al., 1983).

Electrostatics and LBP model

Despite their overall sequence similarity, BPI and LBP differ considerably in their predicted isoelectric points and net charge. Human LBP has an overall charge of −4 (ranging in other species from −4 to +4), while human BPI is +12 (ranging from +12 to +27). In the human proteins, BPI's NH_2-terminal domain (residues 1–230) carries most of the positive charge of the protein (+10), while LBP's NH_2-terminal domain has an overall charge of −4. The COOH-terminal domains of human LBP and BPI are neutral and +2, respectively. Although the above comparisons can be made simply on the basis of sequence data, the three-dimensional structure of BPI offers the first opportunity to map, at least approximately, the locations and distributions of charged residues on LBP. To directly compare the electrostatic surfaces of BPI and LBP, we have constructed a homology model of LBP (described below) using the crystal structure of BPI.

The human BPI and LBP proteins have an overall sequence identity of 45% and can be aligned over their entire length with only two one-residue gaps in LBP (Fig. 1B). Homology modeling between proteins with approximately 50% sequence identity has been shown to produce reasonably accurate models that typically have a backbone RMS deviation (RMSD) of 1.0 Å from crystal structures determined after the models were constructed (Chung & Subbiah, 1996). Each of the one residue gaps in LBP occur in loops or turns of the BPI structure, and therefore should have minimal effect on the overall tertiary structure. Thus, LBP can be expected to share the general structural features of BPI: its elongated shape, pseudosymmetry, the three structural elements (two barrels and central sheet), and also the apolar lipid-binding pockets. Solvent accessibility calculations (Connolly, 1983) indicate that the size of the lipid-binding pocket in the NH_2-terminal domain of the LBP model (607 $Å^2$) is very close to that of the pockets of BPI (Beamer et al., 1997). However, the pocket in the COOH-terminal of LBP domain is considerably smaller (285 $Å^2$). Because these calculations were made using a model of limited accuracy, they should be interpreted with caution. Nevertheless, if the COOH-terminal pocket of LBP cannot accommodate the same ligand as the COOH-terminal pocket of BPI, this could explain some of the functional differences between the COOH-terminal domains of BPI and LBP (mentioned above), as well as differences in complex formation with LPS (Tobias et al., 1997).

The electrostatic surface potentials calculated by GRASP (Nicholls et al., 1991) illustrate the differences in overall charge and charge distribution of the two proteins (Fig. 2C,D). The positive residues (blue) in BPI are generally concentrated near the tip of the NH_2-terminal domain and along the concave face of the boomerang (side of pocket entrances). LBP also has a small area of positive charge near the tip of its NH_2-terminal domain. However, it lacks the distinct positive potential of BPI and has few significantly charged patches on its surface. Despite this overall difference in charge, both BPI and LBP bind to the negatively charged LPS with high affinity ($K_d \sim 10^{-9}$ M), although LBP has an approximately 50-fold lower binding constant (Gazzano-Santoro et al., 1994).

One functional difference between BPI and LBP that might correlate with the difference in charge is bactericidal activity. In one current model for cytotoxicity, the highly cationic BPI is believed to displace the divalent cations, primarily Ca^{2+} and Mg^{2+}, which cross-link the phosphate groups of LPS molecules, in a fashion similar to that which has been shown to occur with the bactericidal peptide polymixin B (Elsbach et al., 1985). Permeability changes in the bacterial membrane (Mannion et al., 1990) suggest that the displacement of these cations breaks apart the lattice of LPS molecules on the bacterial surface, allowing phospholipids from the inner leaflet of the outer membrane to flip into the outer leaflet. Concurrently, the displaced Ca^{2+} ions can bind and activate endogenous phospholipases that degrade the newly accessible phospholipids (Elsbach et al., 1985). While BPI is potently cytotoxic to Gram-negative bacteria, LBP has no detectable bactericidal activity at physiological concentrations (Horwitz et al., 1995). In addition, two lipid transfer proteins (CETP and PLTP) related to BPI and LBP also show high affinity binding to LPS (P.S. Tobias, pers. comm.) (Hailman et al., 1996), but have no known bactericidal activity. Both of these proteins also lack the high net positive charge of BPI. A positively charged peptide derived from residues 85–99 of BPI exhibits bactericidal activity (Little et al., 1994). However, it is not known whether the peptide acts by the same mechanism as the intact protein.

Because of their roles in the innate immune system and LPS-induced inflammatory response, BPI and LBP are of potential interest as therapeutics or targets for inhibitor design. Our recent determination of the structure of human BPI provides the first structural model for this functionally distinctive protein family. An analysis of the conserved residues in the BPI/LBP family reveals that the most highly conserved regions of this protein are involved in forming the lipid-binding pockets, suggesting their functional importance. In addition, our analysis identifies targets for site-directed mutagenesis studies. Together with more and higher resolution crystal structures, these studies should help define the site(s) of LPS interaction and the mechanisms of action of BPI and LBP.

Materials and methods

Sequence alignment

The amino acid sequences of three BPI proteins and four LBP proteins have been published (SWISS-PROT accession numbers: BPI_HUMAN P17213, BPI_BOVIN P17453, BPI_RABIT Q28739, LBP_HUMAN P18428 (Theofan et al., 1994), LBP_RABIT P17454, LBP_MOUSE Q61805, LBP_RAT Q63313). A multiple sequence alignment (Fig. 1B) of these seven sequences was performed using the program CLUSTAL W (Higgins & Sharp, 1989).

Model building

An initial model of LBP was constructed from the BPI coordinates (PDB code 1bp1) using the program HOMOLOGY (Molecular Simulations Inc., San Diego, CA). The sequences of human LBP and BPI were automatically aligned and the side chains of BPI were changed to those of LBP. Two one-residue gaps in LBP (between residues 130–131 and 160–161) were repaired and the resulting structure was energy minimized. The model was visually

inspected, obvious errors corrected, and then subjected to 100 cycles of energy minimization in X-PLOR (Brunger, 1990). The final LBP model has an RMSD for Cα atoms of 0.36 Å with the refined BPI structure. The two additional residues at the COOH-terminus of LBP were modeled as extensions of the final β-strand.

Model quality

Several methods are available for assessing the quality of protein crystal structures and models, and two of these were used to examine the LBP model. The program ERRAT (Colovos & Yeates, 1993) analyzes the statistics of nonbonded interactions between different atom types of proteins, and produces a histogram showing residues with unusual contact statistics (those that fall above an expected 95% confidence limit). In the 2.4 Å BPI model, 93% of the residues lie below the 95% confidence limit. Residues above the limit are concentrated in two regions of the sequence. The first region (residues 143–148) is in a poorly defined loop of barrel N, and several side chains in this area could not be resolved in the electron density maps. The other area (residues 233–248) is in the proline-rich linker between domains of BPI, and also has a number of unresolved side chains. The minimized LBP model has 82% of its residues below this 95% confidence limit. As might be expected, the same areas that were problematic in the BPI structure are also so in the LBP model. Two additional areas with at least a three-residue stretch above the 95% limit are found from residues 71–75 and from 117–120.

The 3D-1D profile method (Bowie et al., 1991) can also be used to assess the local environments of amino acids in a protein structure. A 3D-1D profile is a measure of how compatible a residue is with its environment in the model, based on an analysis of a database of well-refined structures. The program VERIFY3D (Luthy et al., 1992) calculates a score for each residue averaged over a 21-residue sliding window. Low scoring areas of the structure indicate regions with unusual environments, possibly indicating structural errors. In the BPI model, the lowest scoring region occurs around residue 350 and corresponds to a turn between strands of barrel C. Although highly solvent exposed, this area is well defined in the electron density and is not expected to be incorrect. In the LBP profile, the lowest scoring region occurs from residues 230–240 and corresponds to the linker region that also scored poorly in ERRAT. Thus, as assessed by several independent methods, the overall quality of the LBP model appears satisfactory, with the possible exception of residues 230–248.

Acknowledgments

This work was supported by the National Institutes of Health and the Department of Energy. The model of LBP is available upon request from the authors.

References

Abrahamson SL, Wu H-M, Williams RE, Der K, Ottah N, Little R, Gazzano-Santora H, Theofan G, Bauer R, Leigh S, Orme A, Horwitz AH, Carroll SH. 1997. Biochemical characterization of recombinant fusions of lipopolysaccharide-binding protein and bactericidal/permeability-increasing protein: Implications in biological activity. *J Biol Chem 272*:2149–2155.

Beamer LJ, Carroll SF, Eisenberg D. 1997. Crystal structure of human BPI and two bound phospholipids at 2.4 Å resolution. *Science 276*:1861–1864.

Bowie JU, Luethy R, Eisenberg D. 1991. A method to identify protein sequences that fold into a known three-dimensional structure. *Science 253*:164–170.

Brunger AT. 1990. *X-PLOR: A system for crystallography and NMR*. New Haven, Connecticut: Yale University Press.

Camussi G, Montrucchio G, Dominioni L, Dionigi R. 1995. Septic shock—The unraveling of molecular mechanisms. *Nephrol Dial Transplant 10*:1808–1813.

Carson M. 1991. Ribbons 2.0. *J Appl Crystallogr 24*:958–961.

Chung SY, Subbiah S. 1996. A structural explanation for the twilight zone of protein sequence homology. *Structure 4*:1123–1127.

Colovos C, Yeates T. 1993. Verification of protein structures: Patterns of nonbonded contacts. *Protein Sci 2*:1511–1519.

Connolly ML. 1983. Solvent-accessible surfaces of proteins and nucleic acids. *Science 221*:709–713.

Elsbach P, Weiss J. 1995. Prospects for use of recombinant BPI in the treatment of Gram-negative bacterial infections. *Infectious Agents Dis 4*:102–109.

Elsbach P, Weiss J, Kao L. 1985. The role of intramembrane Ca^{2+} in the hydrolysis of the phospholipids of *Escherichia coli* by Ca^{2+}-dependent phospholipases. *J Biol Chem 260*:1618–1622.

Gazzano-Santoro H, Meszaros K, Birr C, Carroll SF, G T, Horwitz AH, Lim E, Aberle S, Kasler H, Parent JB. 1994. Competition between rBPI23, a recombinant fragment of bactericidal/permeability-increasing protein, and lipopolysaccharide (LPS)-binding protein for binding to LPS and gram-negative bacteria. *Infect Immun 62*:1185–1191.

Gazzano-Santoro H, Parent RB, Grinna L, Horwitz A, Parsons T, Theofan G, Elsbach P, Weiss J, Conlon PJ. 1992. High-affinity binding of the bactericidal/permeability-increasing protein and a recombinant amino-terminal fragment to the lipid A region of lipopolysaccharide. *Infect Immun 60*:4754–4761.

Hailman E, Albers JJ, Wolfbauer G, Yu A-Y, Wright SD. 1996. Neutralization and transfer of lipopolysaccharide by phospholipid transfer protein. *J Biol Chem 271*:12172–12178.

Han J, Mathison JC, Ulevitch RJ, Tobias PS. 1994. Lipopolysaccharide (LPS)-binding protein, truncated at Ile-197 binds LPS but does not transfer LPS to CD14. *J Biol Chem 269*:8172–8175.

Higgins DG, Sharp PM. 1989. CLUSTAL: A package for performing multiple sequence alignment on a microcomputer. *Gene 73*:237 244.

Horwitz AH, Williams RE, Nowakowski G. 1995. Human lipopolysaccharide-binding protein potentiates bactericidal activity of human bactericidal/permeability-increasing protein. *Infect Immun 62*:522–527.

Iovine NM, Elsbach P, Weiss J. 1997. An opsonic function of the neutrophil bactericidal/permeability-increasing protein depends on both its N- and C-terminal domains. *Proc Natl Acad Sci USA 94*:10973–10978.

Lamping N, Hoess A, Yu B, Park TC, Kirschning C-J, Pfeil D, Reuter D, Wright SD, Herrmann F, Schumann RR. 1996. Effects of site-directed mutagenesis of basic residues (Arg94, Lys95, Lys99) of lipopolysaccharide (LPS)-binding protein on binding and transfer of LPS and subsequent immune cell activation. *J Immunol 157*:4648–4656.

Little RG, Kelner DN, Lim E, Burke DJ, Conlon PJ. 1994. Functional domains of recombinant bactericidal/permeability increasing protein (rBPI23). *J Biol Chem 268*:1865–1872.

Luthy R, Bowie JU, Eisenberg D. 1992. Assessment of protein models with three-dimensional profiles. *Nature 356*:83–85.

Mannion BA, Weiss J, Elsbach P. 1990. Separation of lethal and sub-lethal effects of the bactericidal/permeability-increasing protein. *J Clin Invest 85*:853–860.

Nicholls A, Sharp KA, Honig B. 1991. Protein folding and association: Insights from the interfacial and thermodynamic properties of hydrocarbons. *Proteins 11*:281–296.

Ooi CE, Weiss J, Doerfler ME, Elsbach P. 1991. Endotoxin-neutralizing properties of the 25 kDa N-terminal fragment and a newly isolated 30 kD C-terminal fragment of the 55-60 kD bactericidal/permeability-increasing protein of human neutrophils. *J Exp Med 174*:649–655.

Pugin J, Schurer-Maly C-C, Leturcq D, Moriarty A, Ulevitch RJ, Tobias PS. 1993. Lipopolysaccharide activation of human endothelial and epithelial cells is mediated by lipopolysaccharide-binding protein and soluble CD14. *Proc Natl Acad Sci USA 90*:2744–2748.

Raetz CR. 1996. Bacterial lipopolysaccharides: A remarkable family of bioactive macroamphiphiles. In: Niedhardt FG, ed. *Escherichia coli and Salmonella: Cellular and molecular biology*. Washington, DC: ASM Press. pp 1035–1063.

Schromm AB, Branderburg K, Rietschel ET, Flad H-D, Carroll SF, Seydel U. 1996. Lipopolysaccharide-binding protein mediates CD14-independent interaction of lipopolysaccharide into phospholipid membranes. *FEBS Lett 399*:267–271.

Theofan G, Horwitz AH, Williams RE, Liu P-S, Chan I, Birr C, Carroll SF, Meszaros K, Parent JB, Kasler H, Aberle S, Trown PW, Gazzano-Santoro H. 1994. An amino-terminal fragment of human lipopolysaccharide-binding protein retains lipid A binding but not CD14-stimulatory activity. *J Immunol 152*:3623.

Tobias PS, Mathison JC, Ulevitch RJ. 1988. A family of lipopolysaccharide-

binding proteins involved in responses to Gram-negative sepsis. *J Biol Chem 263*:13479–12481.

Tobias PS, Soldau K, Iovine NM, Elsbach P, Weiss J. 1997. Lipopolysaccharide (LPS)-binding proteins BPI and LBP for different types of complexes with LPS. *J Biol Chem 272*:18682–18685.

Weiss J, Olson I. 1987. Cellular and subcellular localization of the bactericidal/permeability-increasing protein of neutrophils. *Blood 69*:652–659.

Weiss J, Victor M, Elsbach P. 1983. Role of charge and hydrophobic interactions in the action of the bactericidal/permeability-increasing protein of neutrophils on Gram-negative bacteria. *J Clin Invest 71*:540–549.

Wright SD, Ramos RA, Tobias PS, Ulevitch RJ, Mathison JC. 1990. CD14, a receptor for complex of lipopolysaccharide (LPS) and LPS binding protein. *Science 249*:1431–1433.

Wurfel MM, Kunitake ST, Lichenstein HS, Kane JP, Wright SD. 1994. Lipopolysaccharide (LPS)-binding protein is carried on lipoproteins and acts as a cofactor in the neutralization of LPS. *J Exp Med 180*:1025–1035.